

# Rayleigh-Brillouin Scattering in Binary Gas Mixtures

Z. Gu,<sup>1</sup> W. Ubachs,<sup>1</sup> W. Marques Jr.,<sup>2</sup> and W. van de Water<sup>3</sup>

<sup>1</sup>*Department of Physics and Astronomy, and LaserLab, VU University,  
De Boelelaan 1081, 1081 HV Amsterdam, The Netherlands*

<sup>2</sup>*Departamento de Física, Universidade Federal do Paraná, Caixa Postal 10944, 81531-990, Curitiba, Brazil*

<sup>3</sup>*Physics Department, Eindhoven University of Technology,  
Postbus 513, 5600 MB Eindhoven, The Netherlands*

(Dated: April 12, 2018)

Precise measurements are performed on spectral lineshapes of spontaneous Rayleigh-Brillouin scattering in mixtures of the noble gases Ar and Kr, with He. Admixture of a light He atomic fraction results in marked changes of the spectra, although in all experiments He is merely a spectator atom: it affects the relaxation of density fluctuations of the heavy constituent, but its contribution to the scattered light intensity is negligibly small. The results are compared to a theory for the spectral lineshape without adjustable parameters, yielding excellent agreement for the case of binary monoatomic gases, signifying a step towards modeling and understanding of light scattering in more complex molecular media.

PACS numbers: 42.68.Ca, 42.65.Es, 42.68.Wt, 51.20.+d, 51.40.+p

The spectrum of light scattered in a gas is determined by the fluctuations of its refractive index [1], or, equivalently, by the motion of its molecules. When the mean free path between collisions is much larger than the wavelength, the scattering spectral lineshape is a pure Gaussian, to be understood as a Doppler effect. At higher pressures collisional excitations and acoustic modes come into play, as was recognized independently by Brillouin [2] and Mandelstam [3]. In first approximation, redshifted and blue-shifted frequency components are added to the scattering spectrum with characteristic shifts  $\Delta\nu = v_s k/2\pi$ , with  $v_s$  the speed of sound and  $k$  the size of the scattering wavevector,  $k/2\pi = 2\sin(\theta/2)/\lambda$  with  $\theta$  the scattering angle and  $\lambda$  the wavelength of the incident light.

Rayleigh-Brillouin scattering in dilute gases offers a sensitive probe of gas kinetics. Understanding the scattered light spectrum involves the linearized Boltzmann equation [4], and throughout the years intricate approximations to the collision integral have resulted in various kinetic models for the scattered light spectrum. These models may be viewed as a success of statistical physics. Still, discrepancies with experiments exist, and the kinetic models are generally restricted to simple gases. In contrast, the Earth's atmosphere consists of a mixture of gases, each of which explores internal molecular degrees of freedom. An important practical application of understanding such mixtures of gases is in its connection to laser light scattering (LIDAR) of the atmosphere [5, 6], in particular the ADM-Aeolus mission of the European Space Agency for measuring the global wind profile [7].

The Tenti model is a well-known theory for the spectral lineshape of scattered light in monomolecular gases [8, 9]. The spectrum is determined by the communication between kinetic and internal degrees of freedom, which is characterized by a transport coefficient, the bulk

viscosity  $\eta_b$ . The bulk viscosity is a dynamic quantity, which is not well known at the GHz frequencies of interest in light scattering. Therefore,  $\eta_b$  was used as an adjustable parameter to describe spectral profiles in light scattering in both coherent [10–13] and spontaneous [14–16] Rayleigh-Brillouin scattering experiments. However, the Tenti model is not designed to describe light scattering in mixtures. Nevertheless, applying it to air and assuming that air is a fictitious gas with effective values for its transport coefficients and molecular mass, yields fair agreement with experiments [17, 18]. When devising a proper theory for air, one faces the formidable task of including both kinetic and internal degrees of freedom for several species.

As a first step in understanding light scattering in more complex gases, we will concentrate on mixtures of noble gases using a new experimental setup which provides spectra with unprecedented statistical accuracy [19]. We will compare these spectra to models with no adjustable parameters; the only parameter needed is the atomic diameter, which follows from the well-known value of the shear viscosity of the pure noble gas [20]. All our experiments are in the kinetic regime, where the mean-free path between collisions is comparable to the scattered light wavelength. Interestingly, mixtures of gases with very different mass behave in a similar fashion as a gas of molecules with internal degrees of freedom. While the two components of the mixture briefly can have different temperatures, a molecular gas can have different temperatures associated with translational and internal degrees of freedom. It is the relaxation of these temperature differences that determines the scattered line shape.

The components of our He-Ar and He-Kr mixtures have a large mass disparity ( $M_{\text{He}}/M_{\text{Ar}} = 0.1002$ , and  $M_{\text{He}}/M_{\text{Kr}} = 0.0478$ ). With these different size atoms, it is only the heavy ones that contribute to the scat-

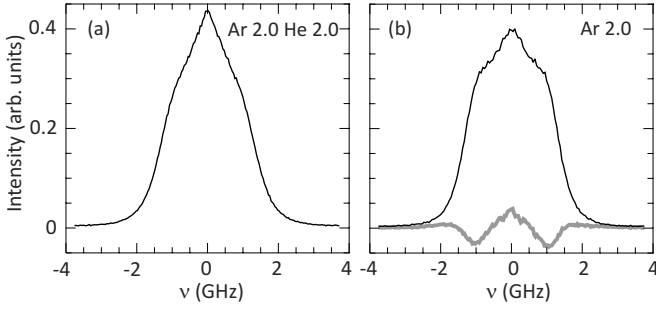


FIG. 1. In He-Ar mixtures, the light He atom acts as a *spectator*, it participates in the gas kinetics, but does not contribute to the scattered light intensity. The spectra of a mixture of 2 bar Ar and 2 bar He (a) is very different from a spectrum of 2 bar Ar (b). The gray line indicates the difference between the spectra.

tered light intensity. The intensity is proportional to the square of the optical polarizabilities  $\alpha$ , with the ratio  $(\alpha_{\text{He}}/\alpha_{\text{Ar}})^2 = 1.56 \times 10^{-2}$ , and  $(\alpha_{\text{He}}/\alpha_{\text{Kr}})^2 = 5.96 \times 10^{-3}$ . Thus, the light atoms are *spectators*, and influence the spectral line shape only indirectly through collisions. Nevertheless, as Fig. 1 illustrates, their influence can be large: adding light atoms to a gas of heavy ones significantly changes the shape of the scattered light spectrum.

A schematic view of the setup for the measurement of spontaneous Rayleigh-Brillouin scattering is shown in Fig. 2. The light from a narrowband continuous-wave laser is scattered off a gas contained in a temperature-controlled gas cell. The laser is a frequency-doubled Ti:Sa laser delivering light at 403 nm, 2 MHz bandwidth and 400 mW of output power. The long-term frequency drift was measured with a wavelength meter to be smaller than 10 MHz per hour. The scattered light is collected at an angle of  $90^\circ$  from an auxiliary focus inside the enhancement cavity, in which a scattering-cell is mounted. The cell is sealed with Brewster windows. The enhancement cavity amplifies the circulating power delivering a scattering intensity of 4 Watt in the interaction region [19]. The light that passes through the FPI is detected using a photo multiplier tube (PMT) which is operated in the photon-counting mode and read out by computer. All measurements are performed at room temperature,  $297 \pm 1$  K.

The scattering angle is determined to be  $90 \pm 0.9^\circ$  by means of the reference laser beam and geometrical relations using sets of diaphragms and pinholes present in the optical setup. The scattered light is filtered by a diaphragm which covers an opening angle of  $2^\circ$ , collected by a set of lenses, further filtered by an extra pinhole ( $d = 50 \mu\text{m}$ ) and then directed into a hemispherical scanning Fabry-Perot interferometer, which is used to resolve the frequency spectrum of the scattered light. To scan the FPI plate distance, the spherical mirror is mounted on a piezo-electrical translator, which is controlled by

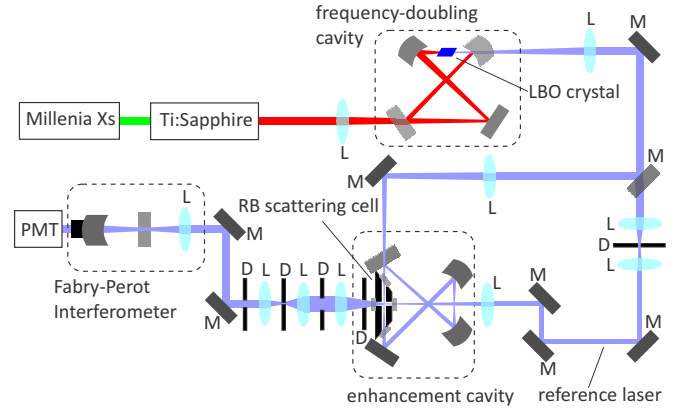


FIG. 2. (Color online) Schematic diagram of the experimental setup for spontaneous Rayleigh-Brillouin scattering. The laser beam (blue line) is amplified in an enhancement cavity to increase the scattering intensity. Scattered light at an angle of  $90^\circ$  is collimated and directed onto a piezo-scannable Fabry-Perot interferometer for spectral analyses, and detected on a photomultiplier tube (PMT).

computer.

The spectral response  $S(\nu)$  of the Fabry-Perot spectrometer was measured in a separate experiment, and could be parametrized very well by the formula  $S(\nu) = [1 + 4(\nu/\nu_w)^2 \text{sinc}^2(\pi\nu/\nu_{\text{FSR}})]^{-1}$ , with  $\text{sinc}(x) = \sin(x)/x$ , and where  $\nu_{\text{FSR}}$  is the free spectral range of the etalon,  $\nu_{\text{FSR}} = 7553$  MHz, and  $\nu_w = 139$  MHz is the Airy-width of the transmission peak. All computed model spectra were convolved with  $S(\nu)$ , and since the free spectral range is relatively small, it is important to allow for the periodic nature of  $S(\nu)$ .

The light scattering experiments do not provide an absolute intensity, therefore the experimental and computed spectra were normalized such that  $\int_{-\nu_b}^{\nu_b} I(\nu) d\nu = 1$ , where the integral extends over one free spectral range (FSR),  $\nu_b = \nu_{\text{FSR}}/2$ . Assuming Poissonian statistics of registered photon counts, an estimate of the statistical error  $\sigma(\nu_i)$  of measured spectra was obtained from the square root of the accumulated photon count  $N_i$  at each discrete frequency  $\nu_i$ . It was verified that the fluctuations  $N_i^{1/2}$  at each  $\nu_i$  were independent. The normalized error is then  $\chi^2 = N^{-1} \sum_{i=1}^N [I_m(\nu_i) - I_e(\nu_i)]^2 / \sigma^2(\nu_i)$ . If the computed line shape model  $I_m$  would fit the measurement perfectly, then only statistical errors remain and the minimum of  $\chi^2$  is unity. The difference between theory and experiment will be expressed by  $\chi^2$ .

In the past decades, many ingenious efforts have been undertaken to arrive at approximate solutions of the Boltzmann equation which are relevant for light scattering. Light scattering involves density fluctuations, with the spectrum of scattered light equalling the Fourier transform of the density-density correlation function. Van Leeuwen and Yip showed that this correlation function follows from the first moment of the solution of the

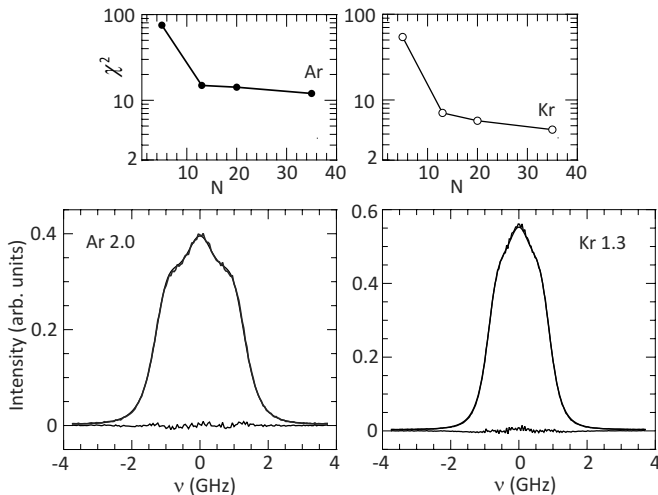


FIG. 3. Comparison of Ar at  $p = 2$  bar and Kr at  $p = 1.3$  bar spectra to the  $N$ -moment model for  $N = 5, 13, 20$  and  $35$ . The spectra are shown for  $N = 35$ , while the convergence with increasing number of moments  $N$  is demonstrated in the top panels.

linearized Boltzmann equation [4].

One such effort is based on the Bhatnagar-Gross-Krook (BGK) model, which takes a simple relaxation form for the collision integral [21],

$$\frac{\partial f}{\partial t} + (\mathbf{c} \cdot \nabla) f = -\sigma (f - f_r), \quad (1)$$

with  $\mathbf{c}$  the molecular velocity,  $f$  the position-velocity distribution function, and  $f_r$  a reference distribution function. The latter is determined from the requirement that  $N$  of its moments are the same as those of the complete collision integral for monatomic particles with a  $r^{-4}$  repulsive interaction potential [22]. Through increasing  $N$ , increasingly accurate predictions of light scattering spectra can be computed. We show this convergence for light scattering in pure samples of Ar and Kr in Fig. 3. These experiments are in the kinetic regime, with uniformity parameter  $y$  of order one. The uniformity parameter  $y$  of a simple gas is the ratio of the scattering wavelength to the mean free path  $l$  between collisions,  $y = 1/(kl)$ . The only information that the theory further needs is the hard-sphere diameter  $a$  of the noble gas atom,  $a_{\text{Ar}} = 3.66 \times 10^{-10}$  m and  $a_{\text{Kr}} = 4.20 \times 10^{-10}$  m. In the case of Ar, the uniformity parameter is  $y_{\text{Ar}} = 1.14$ , while for Kr  $y_{\text{Kr}} = 0.96$ . The  $N = 35$  model can hardly be distinguished from the experimental data. However, since the minimum  $\chi^2$  is still larger than 1, a slight but significant difference between model and experiment remains, although on a relative scale it is  $\lesssim 1\%$ . In fact, the agreement is so good that the model might be viewed as a benchmark testing for experiments. It should be realized, however, that a monatomic ideal noble gas is the simplest system thinkable as there are no internal molecular degrees of freedom.

The BGK-moment approach was used to develop a theory of light scattering in binary mixtures of noble gases [23]. There, the reference distribution function  $f_r$  in Eq. (1) was chosen such as to satisfy the principal conservation properties of the full Boltzmann collision operators, whilst requiring complete correspondence with two-fluid hydrodynamics, i.e. the generalized equations of Navier-Stokes and Fourier. Therefore this model provides a precise transition between the hydrodynamic and kinetic regimes [24]. In this sense, the BGK model with a judicious selection of the reference distribution  $f_r$  allows one to include the relevant physical phenomena in the kinetic description. This is a great advantage for the design of models, as the computation of these various contributions is cumbersome. It is expected that a model that works well for mixtures, no longer works if the density of one of the constituents vanishes, and the gas becomes monatomic. This is because in the design of the mixture model the focus is on inter-species relaxation of temperatures and velocities, and not on the relaxation of high-order gradients that determine the shape of the spectrum of light scattered from monatomic gases.

Measured and computed spectra for light scattering in He-Ar and He-Kr mixtures are shown in Fig. 4. They are characterized by the (partial) pressures and the (partial) uniformity parameters. The definition of the partial uniformity parameters  $y_i = 1/(kl_i)$  of a binary mixture involves the partial mean free paths  $l_i$  of hard-sphere atoms,

$$l_i = \left( \pi \sum_{j=1}^2 n_j a_{ij}^2 \sqrt{1 + M_i/M_j} \right)^{-1}, \quad (2)$$

with  $n_i$  and  $M_i$  the number density and atomic mass of constituent  $i$ , respectively, and  $a_{ij} = (a_i + a_j)/2$  the distance between the centers of two spherical particles with diameters  $a_i$  and  $a_j$  at the instant of collision. With all uniformity parameters of order one, the experiments are in the kinetic regime. The computation of the theory [23] now also needs the hard-sphere diameter of He,  $a_{\text{He}} = 2.16 \times 10^{-10}$  m, and the atomic polarizabilities of the noble gases  $\alpha_{\text{He}} = 0.227 \times 10^{-40}$  Cm<sup>2</sup> V<sup>-1</sup>,  $\alpha_{\text{Ar}} = 1.82 \times 10^{-40}$  Cm<sup>2</sup> V<sup>-1</sup>,  $\alpha_{\text{Kr}} = 2.94 \times 10^{-40}$  Cm<sup>2</sup> V<sup>-1</sup>.

The measured mixture spectra are reproduced well by the theory. Although the mixture model is designed to represent the relevant interspecies relaxation processes, which become less important for asymmetric mixtures, the agreement with the measured spectra at 1 bar He and 3 bars Ar, and the reverse case, is still excellent.

Early experiments on mixtures of He and Xe atoms were done by Clark [25], but were interpreted in terms of hydrodynamics, as a complete kinetic theory was still lacking. Light scattering on He-Xe mixtures in a range of pressures comparable to ours was studied by Letamendia *et al.* [26], and sizable differences with a kinetic mixture model [27] were found.

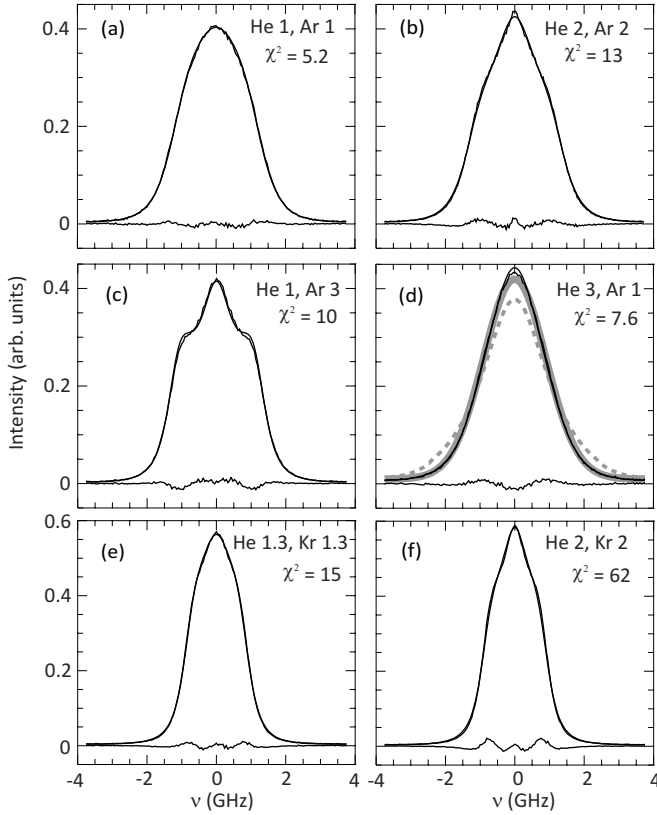


FIG. 4. (Color online) Comparing scattered light spectra of mixtures to the mixture model of [23]. (a) Equimolar mixture He  $p = 1$  bar, Ar  $p = 1$  bar, uniformity parameters  $y_{\text{Ar}} = 1.63$ ,  $y_{\text{He}} = 0.54$ , (b) equimolar mixture He  $p = 2$  bar, Ar  $p = 2$  bar,  $y_{\text{Ar}} = 3.28$ ,  $y_{\text{He}} = 1.08$ , (c) asymmetric mixture He  $p = 1$  bar, Ar  $p = 3$  bar,  $y_{\text{Ar}} = 2.96$ ,  $y_{\text{He}} = 1.16$ , (d) asymmetric mixture He  $p = 3$  bar, Ar  $p = 1$  bar,  $y_{\text{Ar}} = 3.59$ ,  $y_{\text{He}} = 1.00$ , (e) equimolar mixture He  $p = 1.3$  bar, Kr  $p = 1.3$  bar,  $y_{\text{Kr}} = 3.28$ ,  $y_{\text{He}} = 0.77$ , (f) equimolar mixture He  $p = 2$  bar, Kr  $p = 2$  bar,  $y_{\text{Kr}} = 5.01$ ,  $y_{\text{He}} = 1.17$ . The lower line is the difference between experiment and model. Apart from the normalization of the spectra there are no adjustable parameters. In (d), the dashed thick (gray) line shows the Lorentzian spectral lineshape  $I_D$  Eq. (3) with  $D_{\text{He-Ar}}$  the hard-sphere value,  $D_{\text{He-Ar}} = 1.52 \times 10^{-5} \text{ m}^2\text{s}^{-1}$ . The full thick (gray) line (partly obscured) shows the purely Gaussian spectrum of Ar.

A striking observation is the narrowing of the mixture spectrum in Fig. 4(a,d) when the number of helium atoms is increased while keeping the number of Ar atoms the same. Collisional narrowing takes place when for Ar, collisions with He atoms become far more numerous than collisions with another Ar atom. It stands out in the strongly asymmetric mixture of Fig. 4(d). In the kinetic case ( $y_{\text{Ar}} = \mathcal{O}(1)$ ), the spectral lineshape is a Gaussian,  $I(f) \propto \exp(-(2\pi\nu/kv_0)^2)$ , with  $v_0$  the Ar thermal velocity, while in the hydrodynamic limit ( $y_{\text{Ar}} \gtrsim 10$ ), the spectral lineshape is a Lorentzian: the Fourier transform

of the fundamental solution of the diffusion equation,

$$I_D(\nu) = \frac{2D_{\text{He-Ar}}k^2}{(2\pi\nu)^2 + (D_{\text{He-Ar}}k^2)^2}, \quad (3)$$

with  $D_{\text{He-Ar}}$  the mutual He-Ar diffusion coefficient. This collisional narrowing is known as Dicke narrowing [28]; in the hydrodynamic limit it can be explained by the decoherence collisions which an atomic scatterer experiences when it straggles diffusively through a dense gas of spectators. Remarkably, spectral narrowing is manifested here in *non-resonant* light scattering. In our case the partial uniformity parameter evolves from  $y_{\text{Ar}} = 1.6$  at  $p_{\text{He}} = 1$  bar to  $y_{\text{Ar}} = 3.6$  at  $p_{\text{He}} = 3$  bar. Figure 4(d) illustrates that our experimental conditions are still far from the hydrodynamic limit, as the experiment is closer to the Gaussian than to the Lorentzian lineshape. By design, our theory for the lineshape embodies both extreme cases, and it provides a near perfect reproduction of the experimental spectrum.

We have studied Rayleigh-Brillouin scattering in mixtures of noble gases, whose constituents have a very different mass. In all cases, the addition of the light He atomic gas has a large influence on the spectral line shapes, although He atoms hardly contribute to the scattered light intensity. Density fluctuations in mixtures are dominated by the relaxation of temperature and velocity differences between the constituent gases. These relaxations appear to be captured adequately by the mixture model of [23]. This is the first time that these predictions are tested in the kinetic regime. The model contains no adjustable parameters, and reproduces all experiments excellently. The present successful comparison of model and experiment marks a step towards a description of light scattering in mixtures of molecular gases (such as air), and emphasizes the need to account for interspecies relaxation of temperatures of both translational and kinetic degrees of freedom.

- 
- [1] J. W. Strutt (Lord Rayleigh), *Philos. Mag.* **47**, 375 (1899).
  - [2] L. Brillouin, *Ann. d. Phys. (Paris)* **17**, 88 (1922).
  - [3] L. I. Mandelstam, *Zh. Russ. Fiz-Khim.* **58**, 381 (1926).
  - [4] J. M. J. van Leeuwen and S. Yip, *Phys. Rev. A* **139**, 1138 (1965).
  - [5] C. Y. She, R. J. Alvarez, L. M. Caldwell, and D. A. Krueger, *Opt. Lett.* **17**, 541 (1992).
  - [6] B. Witschas, C. Lemmerz, and O. Reitebuch, *Opt. Lett.* **39**, 1972 (2014).
  - [7] O. Reitebuch, C. Lemmerz, E. Nagel, U. Paffrath, Y. Durand, M. Endemann, F. Fabre, and M. Chaloupy, *J. Atmos. Oceanic Technol.* **26**, 2501 (2009).
  - [8] C. D. Boley, R. C. Desai, and G. Tenti, *Can. J. Phys.* **50**, 2158 (1972).
  - [9] G. Tenti, C. D. Boley, and R. C. Desai, *Can. J. Phys.* **52**, 285 (1974).

- [10] J. H. Grinstead and P. F. Barker, Phys. Rev. Lett. **85**, 1222 (2000).
- [11] X. Pan, M. N. Shneider, and R. B. Miles, Phys. Rev. Lett. **89**, 183001 (2002).
- [12] X. Pan, M. N. Shneider, and R. B. Miles, Phys. Rev. A. **71**, 045801 (2005).
- [13] A. S. Meijer, A. S. de Wijn, M. F. E. Peters, N. J. Dam, and W. van de Water, J. Chem. Phys. **133**, 164315 (2010).
- [14] M. O. Vieitez, E. J. van Duijn, W. Ubachs, B. Witschas, A. Meijer, A. S. de Wijn, N. J. Dam, and W. van de Water, Phys. Rev. A **82**, 043836 (2010).
- [15] Z. Gu and W. Ubachs, Opt. Lett. **38**, 1110 (2013).
- [16] Z. Gu, W. Ubachs, and W. van de Water, Opt. Lett. **39**, 3301 (2014).
- [17] Z. Gu, B. Witschas, W. van de Water, and W. Ubachs, Appl. Opt. **52**, 4640 (2013).
- [18] Z. Y. Gu and W. Ubachs, J. Chem. Phys. **141**, 104320 (2014).
- [19] Z. Gu, M. O. Vieitez, E. J. van Duijn, and W. Ubachs, Rev. Scient. Instrum. **83**, 053112 (2012).
- [20] A. Chapman and T. G. Cowling, *Mathematical theory of non-uniform gases* (Cambridge Mathematical library, 1970), 3rd ed., ISBN 052140844.
- [21] P. L. Bhatnagar, E. P. Gross, and M. Krook, Phys. Rev. **94**, 511 (1954).
- [22] W. Marques Jr and G. M. Kremer, Continuum Mech. Thermodyn. **10**, 319 (1998).
- [23] J. R. Bonatto and W. Marques Jr., J. Stat. Mech. **P09014** (2005).
- [24] A. S. Fernandes and W. Marques Jr., Physica A **332**, 29 (2004).
- [25] N. A. Clark, Phys. Rev. A. **12**, 2092 (1975).
- [26] L. Letamendia, P. Joubert, J. P. Chabrat, J. Rouch, C. Vaucamps, C. D. Boley, S. Yip, and S. H. Chen, Phys. Rev. A **25**, 481 (1982).
- [27] C. D. Boley and S. Yip, Phys. of Plasmas **15**, 1424 (1972).
- [28] R. H. Dicke, Phys. Rev. **89**, 472 (1953).